Applied Physics Letters

Solvent-free synthesis of organometallic halides $CH_3NH_3PbI_3$ and $(CH_3NH_3)_3Bi_2I_9$ and their thermoelectric transport properties

Cite as: Appl. Phys. Lett. **115**, 072104 (2019); https://doi.org/10.1063/1.5113535
Submitted: 05 June 2019 . Accepted: 18 July 2019 . Published Online: 13 August 2019

Xiang Long, Zhenyu Pan, Zhuolei Zhang, Jeffrey J. Urban, and Heng Wang

Applied Physics Letters ARTICLE scitation.org/journal/apl

Solvent-free synthesis of organometallic halides $CH_3NH_3PbI_3$ and $(CH_3NH_3)_3Bi_2I_9$ and their thermoelectric transport properties

Cite as: Appl. Phys. Lett. **115**, 072104 (2019); doi: 10.1063/1.5113535
Submitted: 5 June 2019 · Accepted: 18 July 2019 ·
Published Online: 13 August 2019

View Online Export Citation CrossMark

Xiang Long,[1] Zhenyu Pan,[1] Zhuolei Zhang,[2] Jeffrey J. Urban,[2] and Heng Wang[1,a)]

AFFILIATIONS

[1]Department of Mechanical, Materials, and Aerospace Engineering, Illinois Institute of Technology, Chicago, Illinois 60616, USA
[2]The Molecular Foundry, Lawrence Berkeley National Laboratory, Berkeley, California 94720, USA

[a)]heng.wang@iit.edu

ABSTRACT

Organometallic halides are great candidates for optoelectronics. As an important family of semiconductors, understanding their thermoelectric transport properties is also important. This has been a challenging task as many of such compounds are highly intrinsic. In this work, we synthesized two halides, $CH_3NH_3PbI_3$ and $(CH_3NH_3)_3Bi_2I_9$, using a solvent-free method. We found an extraordinarily high Seebeck coefficient of $+2600 \pm 200\ \mu V/K$ in $(CH_3NH_3)_3Bi_2I_9$. For $CH_3NH_3PbI_3$, our synthesis method led to a negative Seebeck coefficient of $-1350 \pm 50\ \mu V/K$, in contrast to positive values observed in solvent synthesized samples. We also found the thermal conductivity of $CH_3NH_3PbI_3$ to be 0.38 W/m K, largely independent of temperature from 300 K to 450 K, despite a tetragonal-to-cubic phase transition. $(CH_3NH_3)_3Bi_2I_9$ has an even lower thermal conductivity of 0.21 W/m K (also temperature independent) which is due to its soft phonon dispersion and weak bonds.

Organometallic halides are a family of emerging semiconductors of great value to optoelectronic applications.[1] Photovoltaic devices using $CH_3NH_3PbI_3$ based materials as absorbers have shown efficiencies over 20% after less than ten years of research.[2] Similar compounds have also demonstrated great performance for other applications such as light emitting diodes,[3] lasers,[4] and sensors.[5] Early studies of photo- and transport physics of $CH_3NH_3PbI_3$ have suggested ultralong minority carrier lifetimes[6] and carrier diffusion lengths,[7] indicating decent carrier mobilities.[8,9] Since ambient condition stability and the use of Pb have drawn increasing concern, researchers are actively searching for other similar compounds (for instance, Pb-free double perovskites[10]), among them is $(CH_3NH_3)_3Bi_2I_9$, which was found[11] to be much more stable under ambient conditions.

Thermoelectrics are semiconductors that make direct conversion between heat and electricity.[12] They can be used for both power harvesting and cooling, with unique advantages such as free of noise and vibration, compactness, and localized cooling. Among other common features, good thermoelectric materials should have (a) low thermal conductivity and (b) high electrical conductivity which require high carrier density and high mobility. Perovskite halides are known to have low thermal conductivities.[13] This makes them naturally of interest in thermoelectric research.

Surprisingly, despite decent mobilities expected in lead halides, it has been rare for the halides to show meaningful thermoelectric performance. Exceptions can only be found in Sn based compounds such as $CH_3NH_3SnI_3$[14] and $CsSnI_3$.[15] $CH_3NH_3PbI_3$ shows great optoelectronic performance, which requires low intrinsic carrier densities. Being able to achieve very low carrier density through the solution process suggests that its defect chemistry does not favor the formation of charged defects. In fact, based on our experience, mixing up to 10% of Sn^{2+} or Bi^{3+} ion in the solution process did not lead to any significant changes in electrical conductivities, such that the samples remain highly insulating preventing any meaningful thermoelectric measurement. However, there is one possibility that has not been explored, that is, the ion equilibrium in and out of solvent might have prevented the formation of charged defects. In fact, defect formation energy calculations[16] on $CH_3NH_3PbI_3$ have suggested that the compound is readily dopable by altering stoichiometry. With this in mind, we designed this study to synthesize the two halides $CH_3NH_3PbI_3$ and $(CH_3NH_3)_3Bi_2I_9$ via a solvent-free method and studied their thermoelectric transport properties. We expect such properties to be drastically different from solution synthesized samples, should the defect chemistry been restricted by solvents. As a result of this study, we confirmed the formation of phase pure halides, and we evaluated their

thermal conductivities and other room temperature thermoelectric properties. Both polycrystalline samples are too insulating to be relevant to thermoelectrics. Nonetheless, the solvent-free synthesis did have some impact on the defect configuration. Exploring it on some similar compounds might create a viable, halide based thermoelectric material.

For the synthesis, we used the method of mechanical alloying via high energy ball milling, followed by hot pressing. Starting materials PbI_2, CH_3NH_3I, and BiI_3 of stoichiometry (total amount around 5 g) were loaded into air-tight 50 ml milling jars and were ball milled with a SPEX shaker mill at room temperature for a short period of time. Phase-pure halide powders were obtained at the end of ball mill, and they were then characterized using XRD, SEM, thermogravimetric analysis (TGA), and reflectance absorption spectroscopy. To obtain bulk samples, the powders were loaded into a graphite dye, which was hot-pressed at 250 °C for 1–2 h. A uniaxial pressure of 40 MPa was applied before heating begins and retrieved during cooling when the sample temperature is below 70 °C; the compacted samples were then free-cooled in the dye. The synthesis and hot-press process were carried out under an inert atmosphere, except when transferring the dye from the glovebox to the hot-press.

Figures 1(a) and 1(b) show the powder X-ray diffraction pattern of $CH_3NH_3PbI_3$ and $(CH_3NH_3)_3Bi_2I_9$. For $CH_3NH_3PbI_3$, a small amount of powder was taken after different amounts of time to monitor phase evolution. The perovskite phase forms very quickly: After 10 min, it is already the majority phase, and after 20 min, no impurity peak can be seen. Similarly, for $(CH_3NH_3)_3Bi_2I_9$, the powder after 30 min has shown a single phase. Many halides can exist in different phases even at the same ambient condition. For a similar compound[17,18] $Cs_3Sb_2I_9$, depending on the synthesis route, it can form either a hexagonal structure with isolated $[Sb_2I_9]^{3-}$ dimers (with edge-sharing SbI_4 octahedra) and surrounding $CH_3NH_3^{1+}$ or one layered structure by "removing" one layer of Sb after every other two layers along the [111] direction of an imaginary perovskite type "$Cs_3Sb_3I_9$." We did not observe this polymorph in $(CH_3NH_3)_3Bi_2I_9$: its XRD pattern is identical to solution synthesized materials: the layered hexagonal structure with isolated dimers.

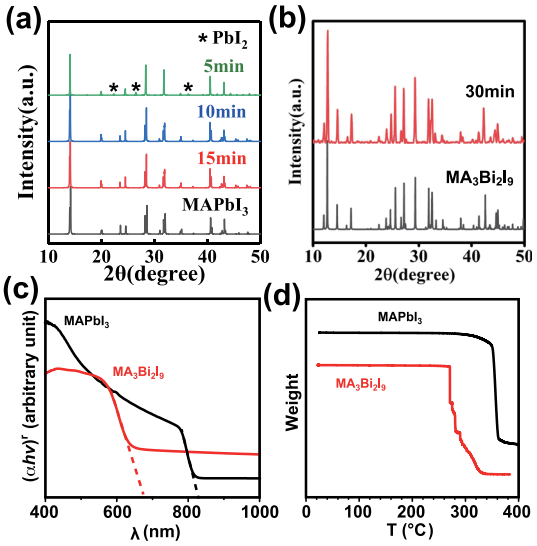

FIG. 1. (a) XRD pattern of $CH_3NH_3PbI_3$ powder after different times of mechanical alloying; reference pattern from PDF 01-085-5509. (b) XRD pattern of $(CH_3NH_3)_3Bi_2I_9$ after 30 min of mechanical alloying; reference pattern from PDF 01-085-6014. (c) Absorption spectrum of the two halides at room temperature. (d) TGA weight loss of the two halides.

Figure 1(c) shows the absorption spectra (Tauc plot) measured with diffusive reflectance on powders. $CH_3NH_3PbI_3$ is a direct bandgap semiconductor, whereas $(CH_3NH_3)_3Bi_2I_9$ has an indirect bandgap; thus, the value of r in $(\alpha h\nu)^r$ is taken as 2 and 0.5 for each compound, respectively. The absorption edges indicated E_g of 1.50 eV (830 nm) for $CH_3NH_3PbI_3$ and 1.82 eV (680 nm) for $(CH_3NH_3)_3Bi_2I_9$, both are in reasonable agreement with the literature result on solution synthesized samples. Figure 1(d) shows the thermogravimetric analysis on powders under Ar flow (heating rate: 3 °C/min). Both halides decompose at relatively low temperatures with the formation of a gaseous phase. For $(CH_3NH_3)_3Bi_2I_9$, this starts sharply at 270 °C, whereas $CH_3NH_3PbI_3$ could maintain >99% of its original weight until 300 °C when weight loss begins. The major decomposition process of $CH_3NH_3PbI_3$ starts at 350 °C.

Both powders are easy to consolidate. We were able to achieve >95% relative densities with cold press of similar pressure. Hot-press was used in order for the grain boundaries to fuse, and so transport properties would not be overwhelmed by grain boundary resistance. Both samples after hot-press were >95% dense but very weak and require extremely careful handling after hot pressing. Figure 2 shows the SEM fracture surfaces of hot pressed pellets. It can be seen from the images of both compounds that fractures propagated almost entirely along grain boundaries, indicating very weak bonding even after hot-press, which is probably due to the lack of liquid phase formation up until very close to decomposition temperatures.

Transport property measurements on most halide perovskites have been very challenging, mostly due to high intrinsic resistivities. This is especially the case for Seebeck coefficient measurements where the true signal is on the order of 0.1 to 1 mV. The low level DC signal measurement requires purposefully designed hardware and electronics, even so the lowest noise level is ultimately limited by Johnson noise. Figure 3(a) illustrates the achievable and prohibited noise levels in the DC voltage measurement for samples with different resistances (figure adapted from Ref. 19). With sample resistance over 10 GΩ, noise between 0.01 and 0.1 mV is close to the theoretical limit. Historically, the only credible Seebeck coefficient measurement[20] on $CH_3NH_3PbI_3$ was performed on a single crystal with resistance on the level of 1 GΩ under room light (other reports exist but likely overwhelmed by artifacts[21]). In this study, we built a measurement system intended for high resistance samples. In addition to attention paid to

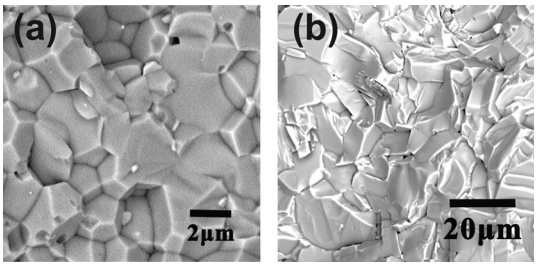

FIG. 2. SEM image of fracture surfaces of hot pressed (a) $CH_3NH_3PbI_3$ and (b) $(CH_3NH_3)_3Bi_2I_9$.

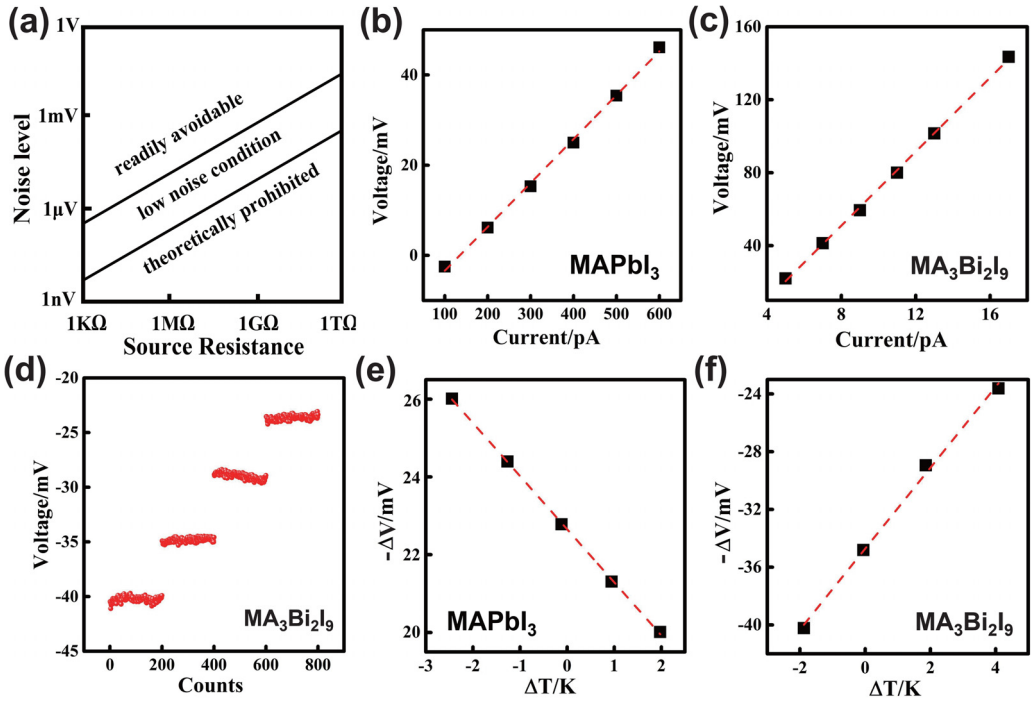

FIG. 3. (a) DC noise voltage levels for DUTs (device under test) with different resistances, Adapted from Ref. 19. Linear four probe I-V curve of (b) $CH_3NH_3PbI_3$ and (c) $(CH_3NH_3)_3Bi_2I_9$. (d) The variation of raw voltage readings for each step during a Seebeck coefficient measurement on $(CH_3NH_3)_3Bi_2I_9$. (e) Seebeck voltage vs temperature difference for $CH_3NH_3PbI_3$. Despite a large offset at $\Delta T = 0$, the slope is linear across positive and negative temperature gradients. The direction of ΔV aligns with ΔT, and so $S = -\Delta V/\Delta T$. (f) The same relation for $(CH_3NH_3)_3Bi_2I_9$.

hardware design, we used a high impedance switch matrix (Keithley 3765) which offers >100 TΩ input impedance through its front-end buffer amplifiers (to ensure meaningful measurement, any meter input impedance should be at least one order of magnitude higher than sample resistance[19]). Our system uses two Peltier devices to generate a temperature gradient. The samples were irregular-shaped slabs with uniform thicknesses (about 0.7 mm), and two tungsten voltage probes were pressed in contact with the surface of the sample through Ga–In liquid metal. Temperature was measured with two miniature K type probes (sheath diameter 1 mm and joint diameter around 0.5 mm) also pressed against sample surfaces in the vicinity of voltage probes. Seebeck voltages were recorded under steady-state conditions. Averages over 200 readings were used. Measurements were carried out in ambient conditions under dark.

Linear four-probe measurements were used to determine the I-V characteristics of both samples [Figs. 3(b) and 3(c)]. The result showed ohmic behavior, which assures proper sample contacts for Seebeck coefficient measurements. The calculated sheet resistance (after geometric correction[22]) is estimated to be on the order of 0.3 GΩ/□ for $CH_3NH_3PbI_3$ and 30 GΩ/□ for $(CH_3NH_3)_3Bi_2I_9$. Resistivities calculated using these values are 20 MΩ cm and 2 GΩ cm. Since the samples are highly resistive, current distributions along the thickness directions are not uniform, and thus, notable error is likely if resistivity was calculated from sheet resistance by dividing the thickness. For such reasons, these listed resistivities should not be viewed as fully quantitative.

Figure 3(d) shows the raw voltage reading in a Seebeck coefficient measurement on $(CH_3NH_3)_3Bi_2I_9$. The I-V curve between two voltage probes is linear with a resistance of 280 GΩ. Despite the extremely high resistance and voltage offset (voltage across two probes when $\Delta T = 0$) on the order of 10 mV, we were still able to record clear, non-drifting voltage steps proportional to temperature differences. Within each temperature step, individual voltage readings vary by up to 2 mV. This fluctuation is close to the theoretical limit shown in Fig. 3(a). Fortunately, the Seebeck signal was large enough for us to determine a room temperature Seebeck coefficient of $+2600 \pm 200\ \mu V/K$ [Fig. 3(f)], from three repeated measurements. Transport theory shows that the Seebeck coefficient increases with decreasing carrier density in a semiconductor, and so one should be able to observe larger Seebeck coefficients in materials that contain fewer carriers. Meanwhile, insulators are considered to have no Seebeck coefficient. This is easy to understand for well-defined semiconductors and insulators, but for materials that fall in the transition region between the two, it remains an interesting question whether they have extraordinary Seebeck coefficients or no Seebeck coefficient at all. On the other hand, even though the Seebeck coefficient has no theoretical limits, what is achievable depends on factors such as defects, which causes a minimum in carrier density and thus a maximum in the Seebeck coefficient. Another factor is the bandgap which limits the maximum possible Seebeck coefficient through the Goldsmid relation[23] ($E_g > 2eS_{max}T_{max}$). Taking Si as an example, the maximum recorded[24] Seebeck coefficient we have found is $-1200\ \mu V/K$ from samples with electron density around $10^{14}\ cm^{-3}$. Of course, as mentioned here, the measurement becomes prohibitively difficult for samples with extreme resistivities.

With all this in mind, it is actually remarkable to observe a Seebeck coefficient greater than 2400 μV/K from the compound of $(CH_3NH_3)_3Bi_2I_9$. This is arguably the highest classic Seebeck coefficient value found in a solid (the classic Seebeck effect due to carrier diffusion, which can be described with Boltzmann transport theory), with the only exception being the so-called colossal Seebeck effect[25] whose physical origin is different and still not well explained (Another Seebeck coefficient analog we should preclude here is the thermovoltage recently observed in electrolyte infiltrated composites[26]). $(CH_3NH_3)_3Bi_2I_9$ achieved such a large value because it has a large bandgap of over 1.8 eV, while maintaining very low charged defect levels, and so the carrier chemical potential is close to the middle of its bandgap.

Figure 3(e) shows measured Seebeck voltage as a function of temperature differences for the compound $CH_3NH_3PbI_3$. The I-V curve between two probes is linear with resistance around 2 GΩ. The measured Seebeck coefficient is -1350 ± 50 μV/K among three repeated measurements. For this specific compound $CH_3NH_3PbI_3$, a very slow settling behavior was seen where the voltage reading drift toward zero over a long period of time (large voltage was applied across the probes for the I-V test and for "preparing" contacts). This phenomenon could be due to (1) slow polarization relaxation through dipole movements or (2) slow ionic diffusion. Fortunately, its impact on the Seebeck measurement can be minimized by waiting for the drift to attenuate. An interesting finding here is the Seebeck coefficient being drastically different from the previously reported value of +900 μV/K measured on a solution-grown single crystal.[20] The difference here indicates that different synthesis methods have a direct impact on the defect configuration in $CH_3NH_3PbI_3$. More specifically, the positive Seebeck coefficient in solution grown $CH_3NH_3PbI_3$ indicates there are more holes. One possible explanation for this is that it is common to use extra CH_3NH_3I during solution synthesis, whereas a strict stoichiometric ratio is used in this work. The abundance of $CH_3NH_3^+$ and I^- could lead to more Pb vacancies, and such vacancies are expected to act as acceptors.

Thermal conductivity of $CH_3NH_3PbI_3$ has been studied experimentally[13,18] and theoretically.[27] For $(CH_3NH_3)_3Bi_2I_9$, there has not been any report on its thermal conductivity. Here, we use the laser flash method to measure thermal diffusivities of polycrystalline samples between 300 and 450 K. Thermal conductivities are calculated from measured thermal diffusivities, densities, and heat capacity (measured with DSC for $(CH_3NH_3)_3Bi_2I_9$, reported values[28] are used for $CH_3NH_3PbI_3$). The result is shown in Fig. 4. We confirmed a low thermal conductivity of 0.38 W/m K for $CH_3NH_3PbI_3$, and we report an

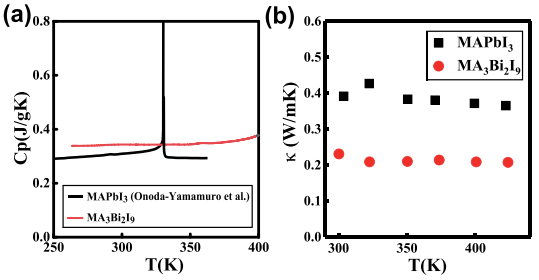

FIG. 4. (a) Measured heat capacity C_p and (b) thermal conductivity as functions of temperature for the two halides.

even lower thermal conductivity of 0.21 W/m K for $(CH_3NH_3)_3Bi_2I_9$. Both values are largely temperature independent, which is common in materials with ultralow thermal conductivities. Thermal conductivity of $CH_3NH_3PbI_3$ has been measured using the steady state method on single crystal and polycrystal samples which revealed[13] very low thermal conductivities: 0.5 W/m K for single crystals and 0.3 W/m K for polycrystals at 300 K. This reported value for the polycrystalline sample is likely an underestimate associated with inherent difficulty of measuring low thermal conductivities using the steady state method. For the same reason, we believe that the reported[29] value of 0.22 W/m K at room temperature from nanowires could also subject to the same error. The same laser flash method was used to measure single crystal $CH_3NH_3PbI_3$ which yielded results that fluctuated between 0.3 and 0.4 W/m K. When measured using the TDTR (time domain thermal reflectance) method, room temperature thermal conductivity in single crystal $CH_3NH_3PbI_3$ was found[30] to be 0.34 W/m K. Measurements[31] on thin film samples using the 3ω method has suggested a room temperature thermal conductivity of 0.33 W/m K. We thus believe the room temperature thermal conductivity of $CH_3NH_3PbI_3$ should be 0.35–0.40 W/m K regardless of being poly-or single crystalline. Meanwhile, the reported[31] temperature dependent measurements on thin films suggested a drastic increase in thermal conductivity to 1.1 W/m K at 350 K as the compound undergoes a phase transition from tetragonal to cubic around 335 K. This is not confirmed by our measurement, which showed no abrupt increase across the phase transition (only a small discontinuity due to measured heat capacity close to phase transition temperature).

Being a hybrid halide with weak metal-halogen bonds, $(CH_3NH_3)_3Bi_2I_9$ has even lower thermal conductivity compared with $CH_3NH_3PbI_3$. This is expected from their crystal structures: $(CH_3NH_3)_3Bi_2I_9$ forms isolated covalently bonded dimmers, whereas $CH_3NH_3PbI_3$ forms a continuous covalent framework.

We have also compared microhardness of these two compounds since it is also related to the strength of bonding and phonon transport. Samples are indented with a diamond Vickers type indenter using loads of 50 or 100 g for $CH_3NH_3PbI_3$ and 25 or 50 g for $(CH_3NH_3)_3Bi_2I_9$. A single crystal of $(CH_3NH_3)_3Bi_2I_9$, grown from its gamma-butyrolactone solution by the antisolvent vapor growth technique, is also included (25 g load). Through multiple measurements, $(CH_3NH_3)_3Bi_2I_9$ consistently showed a very low hardness H_v of 9 ± 0.5 MPa, compared to 55 ± 1 MPa for $CH_3NH_3PbI_3$. The hardness found for the $(CH_3NH_3)_3Bi_2I_9$ single crystal is 10 ± 2 MPa, comparable to the polycrystal. For an intuitive comparison, we also measured the hardness of a sample of phenol formaldehyde resin (a commonly used molding polymer) under the same condition, which is 18 ± 1 MPa, almost twice as high as $(CH_3NH_3)_3Bi_2I_9$. This indicates that the bonds are indeed very soft in $(CH_3NH_3)_3Bi_2I_9$.

To summarize, we synthesized the organometallic halides $CH_3NH_3PbI_3$ and $(CH_3NH_3)_3Bi_2I_9$ by mechanical alloying. The samples obtained are single phase, with sharp absorption edges and bandgaps consistent with their solution synthesized counterparts. Both compounds are insulating, making evaluation of their thermoelectric transport properties very difficult. We managed to evaluate the room temperature Seebeck coefficient of $(CH_3NH_3)_3Bi_2I_9$, which is $+2600 \pm 200$ μV/K. This is among the highest classic Seebeck coefficients ever found in semiconductors. It indicates a Fermi level very close to the middle of the bandgap and extremely low charge carrier levels. On the other hand, we found the Seebeck coefficient of

$CH_3NH_3PbI_3$ to be $-1350 \pm 50\,\mu V/K$, whereas the reported value from a solution grown single crystal was around $+900\,\mu V/K$. This means that when different synthesis routes are used, the charge defect configurations can change. On the thermal transport, we measured the thermal conductivities of $CH_3NH_3PbI_3$ and $(CH_3NH_3)_3Bi_2I_9$ using the laser flash technique to be 0.38 W/m K and 0.21 W/m K at 300 K, both are nearly temperature independent between 300 and 450 K. Microhardness measurements confirmed that $(CH_3NH_3)_3Bi_2I_9$ is a much softer compound even compared to $CH_3NH_3PbI_3$. Even though the two compounds currently are too insulating to be relevant to thermoelectrics, we hope that our work could spur more systematic thermoelectric evaluations on the halide compounds, which could provide useful information regarding their semiconducting nature, as well as insights into better thermoelectric materials.

H.W. and Z.P. acknowledge the start-up support from Illinois Institute of Technology. The work at the Molecular Foundry was supported by the Office of Science, Office of Basic Energy Sciences, of the U.S. Department of Energy and by Lawrence Berkeley National Laboratory under U.S. Department of Energy Contract No. DE-AC02-05CH11231. The authors thank Ian Witting and Professor Jeff Snyder at Northwestern University for their help with hot pressing and thermal conductivity measurements.

REFERENCES

[1]D. B. Mitzi, K. Chondroudis, and C. R. Kagan, IBM J. Res. Dev. **45**(1), 29 (2001); C. C. Stoumpos and M. G. Kanatzidis, Adv. Mater. **28**(28), 5778 (2016); G. Hodes, Science **342**(6156), 317 (2013); D. B. Mitzi, J. Chem. Soc., Dalton Trans. **2001**(1), 1; B. Saparov and D. B. Mitzi, Chem. Rev. **116**(7), 4558 (2016).

[2]A. Kojima, K. Teshima, Y. Shirai, and T. Miyasaka, J. Am. Chem. Soc. **131**(17), 6050 (2009); H. S. Kim, C. R. Lee, J. H. Im, K. B. Lee, T. Moehl, A. Marchioro, S. J. Moon, R. Humphry-Baker, J. H. Yum, J. E. Moser, M. Gratzel, and N. G. Park, Sci. Rep. **2**, 591 (2012); J. Burschka, N. Pellet, S. J. Moon, R. Humphry-Baker, P. Gao, M. K. Nazeeruddin, and M. Gratzel, Nature **499**(7458), 316 (2013); W. S. Yang, J. H. Noh, N. J. Jeon, Y. C. Kim, S. Ryu, J. Seo, and S. Il Seok, Science **348**(6240), 1234 (2015).

[3]Z. K. Tan, R. S. Moghaddam, M. L. Lai, P. Docampo, R. Higler, F. Deschler, M. Price, A. Sadhanala, L. M. Pazos, D. Credgington, F. Hanusch, T. Bein, H. J. Snaith, and R. H. Friend, Nat. Nanotechnol. **9**(9), 687 (2014).

[4]G. Xing, N. Mathews, S. Sien Lim, N. Yantara, X. Liu, D. Sabba, M. Grätzel, S. Mhaisalkar, and T. Chien Sum, Nat. Mater. **13**, 476 (2014); H. Zhu, Y. Fu, F. Meng, X. Wu, Z. Gong, Q. Ding, M. V. Gustafsson, M. T. Trinh, S. Jin, and X. Y. Zhu, Nat. Mater. **14**(6), 636 (2015).

[5]X. Hu, X. Zhang, L. Liang, J. Bao, S. Li, W. Yang, and Y. Xie, Adv. Funct. Mater. **24**(46), 7373 (2014).

[6]R. E. Brandt, V. Stevanović, D. S. Ginley, and T. Buonassisi, MRS Commun. **5**(2), 265 (2015).

[7]Q. Dong, Y. Fang, Y. Shao, P. Mulligan, J. Qiu, L. Cao, and J. Huang, Science **347**(6225), 967 (2015); S. D. Stranks, G. E. Eperon, G. Grancini, C. Menelaou, M. J. P. Alcocer, T. Leijtens, L. M. Herz, A. Petrozza, and H. J. Snaith, *ibid.* **342**(6156), 341 (2013); R. L. Milot, G. E. Eperon, H. J. Snaith, M. B. Johnston, and L. M. Herz, Adv. Funct. Mater. **25**(39), 6218 (2015).

[8]J. M. Frost, K. T. Butler, F. Brivio, C. H. Hendon, M. van Schilfgaarde, and A. Walsh, Nano Lett. **14**(5), 2584 (2014).

[9]T. M. Brenner, D. A. Egger, A. M. Rappe, L. Kronik, G. Hodes, and D. Cahen, J. Phys. Chem. Lett. **6**(23), 4754 (2015).

[10]G. Volonakis, M. R. Filip, A. A. Haghighirad, N. Sakai, B. Wenger, H. J. Snaith, and F. Giustino, J. Phys. Chem. Lett. **7**(7), 1254 (2016).

[11]B. W. Park, B. Philippe, X. Zhang, H. Rensmo, G. Boschloo, and E. M. Johansson, Adv. Mater. **27**(43), 6806 (2015).

[12]L. E. Bell, Science **321**(5895), 1457 (2008).

[13]A. Pisoni, J. Jacimovic, O. S. Barisic, M. Spina, R. Gaal, L. Forro, and E. Horvath, J. Phys. Chem. Lett. **5**(14), 2488 (2014).

[14]Y. Takahashi, R. Obara, Z. Z. Lin, Y. Takahashi, T. Naito, T. Inabe, S. Ishibashi, and K. Terakura, Dalton Trans. **40**(20), 5563 (2011); Y. Takahashi, H. Hasegawa, Y. Takahashi, and T. Inabe, J. Solid State Chem. **205**, 39 (2013); F. Hao, C. C. Stoumpos, D. Hanh Cao, R. P. H. Chang, and M. G. Kanatzidis, Nat. Photonics **8**(6), 489 (2014).

[15]W. Lee, H. Li, A. B. Wong, D. Zhang, M. Lai, Y. Yu, Q. Kong, E. Lin, J. J. Urban, J. C. Grossman, and P. Yang, Proc. Natl. Acad. Sci. U. S. A. **114**(33), 8693 (2017); I. Chung, J. H. Song, J. Im, J. Androulakis, C. D. Malliakas, H. Li, A. J. Freeman, J. T. Kenney, and M. G. Kanatzidis, J. Am. Chem. Soc. **134**(20), 8579 (2012).

[16]W.-J. Yin, T. Shi, and Y. Yan, Appl. Phys. Lett. **104**(6), 063903 (2014); A. Buin, P. Pietsch, J. Xu, O. Voznyy, A. H. Ip, R. Comin, and E. H. Sargent, Nano Lett. **14**(11), 6281 (2014).

[17]K. Yamada, H. Sera, S. Sawada, H. Tada, T. Okuda, and H. Tanaka, J. Solid State Chem. **134**(2), 319 (1997); B. Saparov, F. Hong, J.-P. Sun, H.-S. Duan, W. Meng, S. Cameron, I. G. Hill, Y. Yan, and D. B. Mitzi, Chem. Mater. **27**(16), 5622 (2015); A. J. Lehner, D. H. Fabini, H. A. Evans, C.-A. Hébert, S. R. Smock, J. Hu, H. Wang, J. W. Zwanziger, M. L. Chabinyc, and R. Seshadri, Chem. Mater. **27**(20), 7137 (2015).

[18]J.-H. Chang, T. Doert, and M. Ruck, Z. Anorg. Allg. Chem. **642**(13), 736 (2016).

[19]https://www.tek.com/document/handbook/low-level-measurements-handbook.

[20]T. Ye, X. Wang, X. Li, A. Q. Yan, S. Ramakrishna, and J. Xu, J. Mater. Chem. C **5**(5), 1255 (2017).

[21]X. Mettan, R. Pisoni, P. Matus, A. Pisoni, J. Jaćimović, B. Náfrádi, M. Spina, D. Pavuna, L. Forró, and E. Horváth, J. Phys. Chem. C **119**(21), 11506 (2015); C. C. Stoumpos, C. D. Malliakas, and M. G. Kanatzidis, Inorg. Chem. **52**(15), 9019 (2013).

[22]S. M. Sze, *Semiconductor Devices: Physics and Technology* (John Wiley and Sons, Singapore, 2012).

[23]Z. M. Gibbs, H.-S. Kim, H. Wang, and G. Jeffrey Snyder, Appl. Phys. Lett. **106**(2), 022112 (2015).

[24]G. A. Slack and M. A. Hussain, J. Appl. Phys. **70**(5), 2694 (1991).

[25]A. Bentien, S. Johnsen, G. K. H. Madsen, B. B. Iversen, and F. Steglich, Europhys. Lett. **80**(1), 17008 (2007); D. Byeon, R. Sobota, K. Delime-Codrin, S. Choi, K. Hirata, M. Adachi, M. Kiyama, T. Matsuura, Y. Yamamoto, M. Matsunami, and T. Takeuchi, Nat. Commun. **10**(1), 72 (2019).

[26]T. Li, X. Zhang, S. D. Lacey, R. Mi, X. Zhao, F. Jiang, J. Song, Z. Liu, G. Chen, J. Dai, Y. Yao, S. Das, R. Yang, R. M. Briber, and L. Hu, Nat. Mater. **18**(6), 608 (2019).

[27]T. Hata, G. Giorgi, and K. Yamashita, Nano Lett. **16**(4), 2749 (2016); X. Qian, X. Gu, and R. Yang, Appl. Phys. Lett. **108**(6), 063902 (2016).

[28]N. Onoda-Yamamuro, T. Matsuo, and H. Suga, J. Phys. Chem. Solids **51**(12), 1383 (1990).

[29]Y. Wang, R. Lin, P. Zhu, Q. Zheng, Q. Wang, D. Li, and J. Zhu, Nano Lett. **18**(5), 2772 (2018).

[30]G. A. Elbaz, W. L. Ong, E. A. Doud, P. Kim, D. W. Paley, X. Roy, and J. A. Malen, Nano Lett. **17**(9), 5734 (2017).

[31]R. Heiderhoff, T. Haeger, N. Pourdavoud, T. Hu, M. Al-Khafaji, A. Mayer, Y. Chen, H.-C. Scheer, and T. Riedl, J. Phys. Chem. C **121**(51), 28306 (2017).